High-Resolution Long-Term Trends in Relative Abundance from Spatial Modeling of Audubon Christmas Bird Counts

Timothy D. Meehan[1], Nicole L. Michel[2], and Håvard Rue[3]

[1] *National Audubon Society, Boulder, Colorado, USA*

[2] *National Audubon Society, Portland, Oregon, USA*

[3] *King Abdulla University of Science and Technology, Thuwal, Saudi Arabia*

Abstract

Bird counts by community volunteers provide valuable information about the conservation needs of many bird species. The statistical modeling techniques commonly used to analyze these counts provide robust, long-term trend estimates from heterogeneous community science data at regional, national, and continental scales. Here we present a different modeling approach that increases the spatial resolution of trend estimates, and reduces the computational burden of trend estimation, each by an order of magnitude. We demonstrate the approach with data for the American Robin (*Turdus migratorius*) from Audubon Christmas Bird Counts conducted between 1966 and 2017. We show that aggregate regional trend estimates from the proposed method align well with those from the current standard method, and that spatial variation in trends are associated with winter temperatures and human population densities as expected from the avian energetics literature. It appears that the proposed technique can provide reasonable large-scale trend estimates for users concerned with general patterns, while also providing higher resolution

estimates for others examining correlates of abundance trends at finer spatial scales, which is a prerequisite for tailoring management plans to local conditions.

Key Words

Audubon Christmas Bird Count, Bayesian hierarchical model, North American Breeding Bird Survey, population trends, spatially varying coefficients, conditional autoregressive model

Introduction

Volunteers with the Audubon Christmas Bird Count (CBC) have been counting wintering birds across North America every year for the last 118 years (Dunn et al. 2005, Soykan et al. 2016). Population trends derived from CBC data, along with those derived from other large-scale monitoring programs like the North American Breeding Bird Survey (BBS, Robbins et al. 1989, Sauer et al. 2017), provide valuable information for understanding the conservation needs of North American bird species (Dickinson et al. 2010, Hochachka et al. 2012). For example, CBC and BBS trends are used to evaluate population change rates and population half-lives for many of the 448 bird species included in the Partners in Flight Landbird Conservation Plan (Rosenberg et al. 2016, 2017). CBC and BBS trends are also used by BirdLife International (http://datazone.birdlife.org/species/search) to make status recommendations to the International Union for Conservation of Nature, creators of the Red List of Threatened Species (https://www.iucnredlist.org/). CBC trends are especially useful for species who are otherwise not monitored in their remote northern breeding locations (Niven et al. 2004).

The current, standard approach for generating trends from CBC data (Link et al. 2006, Soykan et al. 2016) was derived from methods originally developed for BBS data (Link and

Sauer 2002, Sauer and Link 2011). The general approach is to assign counts in Canada and the US to one of up to 169 polygons or spatial strata, which are intersections of US states, Canadian provinces, and Bird Conservation Regions (BCR, Sauer et al. 2003). Then, treating each stratum as independent, a non-linear function is used to correct for the effect of observer effort on counts, while simultaneous effects are estimated for the impact of count circle, year, and stratum by year (Link et al. 2006, Soykan et al. 2016). These parameter estimates are used to derive a relative abundance index per stratum and year, and those indices are used to compute annual percent change per stratum across defined time periods (Link and Sauer 2002, Sauer and Link 2011).

The standard CBC analysis provides robust long-term trend estimates from heterogeneous community science data across large spatial scales. By pooling count circles per stratum, this approach deals with the issue of count circles haphazardly becoming active or inactive over the time series (Sauer and Link 2011, Soykan et al. 2016). Additionally, pooling produces a sufficiently large sample of counts to generate a reasonably robust count-effort correction function (Link and Sauer 1999), which is critical given the wide variation in count effort among count circles (Bock and Root 1981, Dunn et al. 2005). This approach produces a relative abundance index per year and stratum, which can be used to explore variation around long-term log-linear trends, and can be summed across larger hierarchically nested strata, such as states, provinces, or BCRs, and used to calculate change in relative abundance at larger spatial scales. Producing annual abundance indices also permits summarizing abundance change between any desired pair of time points. Finally, the simplicity of the standard model enables a flexible and robust computational process, suitable for analysis of hundreds of species that vary enormously in their ubiquity, abundance, and population dynamics.

While the current approach produces trends that are useful for understanding population status of birds at regional to continental scales, the approach has some limitations. As implemented, it is a computationally intensive process, especially for wide-ranging species. This is due to the use of Markov chain Monte Carlo (MCMC) to estimate model parameters for relative abundance, and processing large MCMC chains to scale relative abundance to larger aggregate units to generate change estimates. Additionally, their coarse resolution limits their ability to provide inference about local variation and processes. While trends can be scaled up to larger spatial units, they cannot be scaled down to smaller ones. The analytical stratum is the finest level of resolution, which limits the extent to which variation in trends can be attributed to processes occurring at finer spatial scales (Thogmartin et al. 2004, Bled et al. 2013) and limits possibilities for tailoring conservation plans to local conditions (Ethier and Nudds 2015, Ethier et al. 2017).

Moreover, the current approach does not take full account or advantage of spatial relationships among counts. Modeling this structure would facilitate borrowing information across spatial boundaries, allowing more robust trend estimates in places where data are sparse (Waller and Gotway 2004, Blangiardo et al. 2013, Banerjee et al. 2014). Indeed, borrowing of information could possibly allow trends to be estimated at spatial scales that are finer than the spatial strata currently used (Thogmartin et al. 2004, Bled et al. 2013). Accounting for the spatial dependence across count sites also reduces the amount of spatial autocorrelation in model residuals, which leads to more reliable inference about trend estimates (Dormann et al. 2007, Beale et al. 2010).

Previous work by Thogmartin et al. (2004), Bled et al. (2013), and Smith et al. (2015), among others, offered spatially-explicit variations of the standard trend analysis approach for

community science data. These works were focused on analysis of BBS data, but their approaches are easily related to analysis of CBC data. Instead of using the standard strata described above (Smith et al. 2015), Thogmartin et al. (2004) assigned count sites to irregular polygons, created by tessellation of BBS route locations. Bled et al. (2013) assigned routes to cells on a regular grid, with one-degree latitude and longitude spacing. All three studies utilized spatially-structured random intercepts for relative abundance per polygon, grid cell, or stratum. Thogmartin et al. (2004) utilized a fixed effect of year per polygon, but that effect did not incorporate spatial structure. Bled et al. (2013) and Smith et al. (2015) estimated relative abundances per year, and then trends were generated as derived parameters, as done in the standard analysis.

Here, we present a different approach for calculating temporal trends in relative abundance, one that takes advantage of the considerable spatial structure in CBC data. This approach borrows components from previous ones, incorporates new components that prioritize robust trend estimation at finer spatial scales, and employs a simplified and computationally efficient workflow. Similar to Bled et al. (2013), we assigned CBC count sites to cells on a uniform grid that covered North America. In contrast to previous work, effort and year effects were modeled as random slopes with spatial structure, following a spatially varying coefficient (SVC) approach (Gelfand et al. 2003, Finley 2011, Congdon 2014). Finally, unlike prior studies using MCMC, we used integrated nested Laplace approximation (INLA) to estimate Bayesian posteriors for model parameters (Lindgren and Rue 2015, Rue et al. 2017), which led to a dramatic decrease in computing time. The four goals of this report were to (*i*) describe an SVC approach to calculating trends in CBC data, (*ii*) employ the approach using data for the American Robin, (*iii*) compare trend results derived from the SVC approach to aggregate results derived

from standard methods, and (*iv*) demonstrate use of fine scaled trend results through a simple analysis exploring correlations between SVC trends and potential energetic drivers related to climate and winter food resources.

Methods

Christmas Bird Count

We demonstrate use of the SVC approach using data from the CBC, a volunteer bird monitoring program begun in 1900. Since its inception, the program has grown tremendously, and now includes more than 2,400 count sites and involves more than 70,000 volunteers (Soykan et al. 2016). The program extends across North and South America, but the majority of counts have been conducted in the US and Canada. The program has produced counts extending 118 years, but standard trend analyses are conducted using counts conducted after 1965, as protocols and count efforts have been most consistent since then. An individual CBC occurs over a 24-hour period, once per year, during late December or early January. During a count, volunteers record birds seen or heard within a circular study area with a 24.1 km diameter. The area covered and the amount of time spent counting birds in a given circle varies considerably across years and count locations, so annual effort metrics are recorded and used to standardize bird counts. More details about the CBC can be found in Bock and Root (1981) and Dunn et al. (2005), who describe the program and discuss the potential uses and limitations of CBC data.

Statistical model

We modeled CBC count data, $y_{i,k,t}$, for grid cell *i* encompassing count circle *k* during year *t*, as a random variable from a negative binomial distribution. Expected values for counts per grid cell,

$\mu_{i,t}$, were assumed to be a function of spatially-structured grid-cell, count-effort, and year effects, plus unstructured variation among count circles. The linear predictor for $\mu_{i,t}$ took the form

$$\log(\mu_{i,t}) = \alpha_i + \epsilon_i \log(E_{i,k,t}) + \tau_i T_{i,k,t} + \kappa_k. \quad \text{(Eq. 1)}$$

Parameters α_i were modelled as cell-specific random intercepts with an intrinsic conditional autoregressive (CAR) structure (Besag et al. 1991). With this structure, α_i values came from a normal distribution, with a conditional mean related to the average of adjacent cells, and with conditional variance proportional to the variance across adjacent cells and inversely proportional to the number of adjacent cells. Spatial structure was incorporated into α_i to allow for information about relative abundance to be shared across neighboring cells, and to reduce the spatial autocorrelation among model residuals that occurs when this spatial structure is ignored (Dormann et al. 2007, Finley 2011).

Parameters ϵ_i were modeled as spatially-structured, cell-specific, random slope coefficients for the effort effect. These spatially varying coefficients (Gelfand et al. 2003, Banerjee et al. 2014, Congdon 2014) were also modelled with a CAR structure (Besag et al. 1991). Slopes were drawn from a normal distribution with a conditional mean related to the average of adjacent cells, and with conditional variance proportional to the variance across adjacent cells and inversely proportional to the number of adjacent cells. Spatial structure was incorporated into ϵ_i to allow for information about the effort effect to be shared across neighboring cells, and to accommodate a potential lack of stationarity in the effort effect (Finley 2011). Effort was represented by $E_{i,j,k}$, the number of party hours expended during a count,

where a party hour was the count effort of one party of unspecified size for one hour. Pairing log-transformed counts with log-transformed effort in the linear predictor yielded a power function for effort correction, a flexible mathematical form that accommodated a decreasing, linear, or increasing impact of effort on expected counts (Butcher and McCulloch 1988, Link and Sauer 1999).

Parameters τ_i were modeled as spatially-structured, cell-specific, random slope coefficients for the year effect. Spatially varying τ_i coefficients (Gelfand et al. 2003, Banerjee et al. 2014, Congdon 2014) were also modeled with CAR structure (Besag et al. 1991), where values came from a normal distribution, with conditional means and variances as described above. Spatial structure was incorporated into τ_i to allow for information about the year effect to be shared across neighboring cells, and to allow the year effect to vary across the cells in the study region. Year, represented by *T*, was transformed before analysis such that max(*T*) = 0, and each preceding year took an increasingly-negative integer value. Given the scaling of effort and year variables, $\exp(\alpha_i)$ could be interpreted as a cell-specific expected count given one party hour of effort during the final year in the time series.

The final term in the model, κ_k, was an exchangeable random effect that accounted for variation in relative abundance among circles, possibly due to differences in habitat conditions or observer experience (Soykan et al. 2016). Note that the model did not include a normally-distributed, observation-level random effect to deal with overdispersed Poisson counts, i.e., $y \mid \varepsilon \sim \text{Poisson}(\mu\varepsilon)$ and $\varepsilon \sim \text{normal}(\mu, \sigma)$, as is done for the standard approach (Sauer and Link 2011, Soykan et al. 2016). Rather, we used a negative binomial count distribution for *y*, i.e., $y \mid \varepsilon \sim \text{Poisson}(\mu\varepsilon)$ and $\varepsilon \sim \text{gamma}(\phi^{-1}, \phi^{-1})$ (Linden and Mantyniemi 2011). These two approaches are expected to yield similar outcomes. However, as implemented in R-INLA, the

latter approach returns a single dispersion estimate while foregoing estimation of individual observation effects, which reduces computing time and the size of posterior samples.

Case Study Data

We developed a case study, using data for the American Robin (*Turdus migratorius*) from CBCs conducted across the continental US and Canada between 1966 and 2017, to demonstrate the SVC modeling approach, compare results with those from the standard approach, and illustrate a straightforward analysis of fine scaled trends. Before modeling the CBC data, extreme outliers (> 3 SD from the mean, after log transformation) in counts and effort were removed. After filtering, there were 36,650,191 American Robins encountered in 78,140 counts from 3,195 count circles over 52 years, for modeling.

Locations of the 3,195 unique count circles were mapped using the North American Albers Equal Area Conic projection (EPSG 102008, https://epsg.io/102008) and assigned to 880 cells on a grid divided along 100 km increments in latitude and longitude (Fig. 1A). Grid cells formed a continuous lattice within a non-convex polygon created using circle locations. The number of count circles per grid cell varied from 0 to 20, and averaged 2.43 (Fig. 1A). The number of neighbors for a given grid cell ranged from 1 to 8, and averaged 7.48. Note that grid cells with zero counts were retained during model estimation to preserve the spatial relationships between counts. However, before analyzing resulting trend estimates, cells with no observed counts were removed from the dataset, as we were not interested in interpolated trends for grid cells without CBC sites.

Model Computation

The SVC model described above was analyzed within a Bayesian framework using the R-INLA package (Rue et al. 2017) for R statistical computing software (R Core Team 2016). For parameters α_i, ϵ_i, and τ_i, with CAR structure, precision matrices were scaled such that the geometric mean of marginal variances was equal to one (Riebler et al. 2016), and priors for precision parameters were penalized complexity (PC) priors, with parameter values $U_{pc} = 1$ and $a_{pc} = 0.01$ (Simpson et al. 2017). Precision for the zero-centered, exchangeable, random circle effect, κ_k, was also assigned a PC prior with parameter values $U_{pc} = 1$ and $a_{pc} = 0.01$ (Simpson et al. 2017). The overdispersion term for the negative binomial count distribution, ϕ, was assigned a PC prior with parameter value $l = 7$. Very simply, as implemented here, PC priors were weakly informative priors with an innate tendency to shrink structured and unstructured random effects toward zero in the absence of a strong signal. Readers are referred to Simpson et al. (2017) for the details of, and rationale behind, PC priors, as well as the default structures and parameter values of PC priors used in the R-INLA package.

Along with parameter estimates, R-INLA produced two values to evaluate individual model fit (Czado et al. 2009) and compare different models to one another (Gneiting and Raftery 2007, Link et al. 2017): cross-validation probability integral transform (PIT, Dawid 1984) and conditional predictive ordinate (CPO, Pettit 1990). For this application, we were not comparing multiple models. However, we extracted PIT values and visually inspected their histogram, as an approximate uniform distribution is expected for a model that fits the data reasonable well (Czado et al. 2009, Held et al. 2010).

Following model analysis, posterior medians and symmetric 95% credible intervals were computed per cell for α_i, ϵ_i, and τ_i. Credible interval widths, representing estimate uncertainty, were computed by subtracting the lower credible limit from the upper credible limit per cell.

Posterior summaries were then mapped to visualize spatial variation in abundance indices, effort effects, and relative-abundance trends.

Trend Comparisons

It is common, following CBC and BBS analyses, to aggregate trend information to larger scales that might be of interest to resource managers designing and implementing policies across states, provinces, BCRs, or nations (Sauer et al. 2003, Sauer and Link 2011, Soykan et al. 2016). After analysis of the SVC model for American Robin, we aggregated 100 km results to the BCR level in order to compare them to those produced using standard CBC analysis methods (Soykan et al. 2016). SVC trends were aggregated for each BCR by averaging trends for all equal-area grid cells where the cell centroid fell within the BCR. We evaluated the uncertainty around SVC trend estimates by comparing credible interval widths for cells within a BCR to those calculated for a BCR using the standard approach. We note that full posterior distributions for aggregate SVC trend estimates could have been computed by averaging random draws from τ_i posteriors for cells within a BCR, or by using R-INLA functions for creating linear combinations (Blangiardo et al. 2013). Further, those averages could have been weighted by the amount of area where the cells and BCR overlap (Bled et al. 2013). We did not employ these methods here because our main focus was on fine scale trends and only qualitative comparison with standard results.

Analysis of Preprocessed Trends

Dunn et al. (2005) suggested that analyses of CBC data by the broader scientific community would increase in number and quality as preprocessed effort-corrected trends were made

available to the public, as they have been for the BBS results (Sauer et al. 2003). Work by Soykan et al. (2016) marks the initial outcome of an effort by Audubon to make this happen, and standard trend analysis results have recently become publically available via the internet for over 500 species (https://www.audubon.org/conservation/where-have-all-birds-gone). It is possible that SVC trends could also become publically available for researchers interested in exploring factors associated with preprocessed, fine-scaled trends. Given this potential, we conducted a simple demonstration analysis of fine scaled American Robin trends.

Specifically, we explored correlations between SVC abundance trends and latitude, minimum winter temperature, and human population density. We expected that, in the Northern Hemisphere, latitude would be positively related to SVC trends, as several landbird species appear to be shifting their ranges towards the Earth's poles (Thomas and Lennon 1999, La Sorte and Thompson 2007). A northward range shift would logically lead to negative trends in the southern portion of their range and positive trends in the northern portion of their range. One putative mechanism for northward range shifts in wintering birds is the increase in minimum winter temperatures across the continent over the past 50 years (Zuckerberg et al. 2011, Princé and Zuckerberg 2015), which makes the energetics of wintering in the north more favorable (Root 1988, Meehan et al. 2004). With this mechanism in mind, we expected that, for a given latitude, residual trends would be negatively related to minimum winter temperature, as birds began wintering in historically colder locations further from coasts and higher in elevation. Finally, we tested the hypothesis that winter bird distribution is also governed by resource availability (Dunning and Brown 1982, Meehan et al. 2004). We expected that, after accounting for latitude and minimum winter temperature, SVC trends would be positively related to human population density (Robb et al. 2008, Zuckerberg et al. 2011), as American Robins are well

known to prosper in human dominated landscapes, replete with mown grass, fruiting ornamentals, and bird feeders (Beissinger and Osborne 1982, Marzluff 1997).

For this analysis, τ_i values were related to the latitude of the centroid for a given 100 km grid cell. Average minimum December and January temperature was calculated per cell between 1965 and 2017, using the CRU TS v4.01 dataset (Harris et al. 2014). Average human population size between 1970 and 2015 was calculated per cell using Global Population Count Grid Time Series Estimates (CIESIN 2017) for 1970 and the GPWv4 (CIESIN 2016) dataset for 2015. Cell specific τ_i values were modeled with a latent Gaussian model, where $\tau_i \sim \text{Normal}(\mu_i, \sigma^2)$, $\mu_i = \beta_0 + \beta_1 L_i + \beta_2 T_i + \beta_3 (P_i^{0.25}) + \upsilon_i$, and L_i, T_i, and P_i represented cell-specific latitude, average minimum winter temperature, and average human population size variables, respectively. Note the transformation of P_i, which was highly right-skewed. The term υ_i represented cell-specific random intercepts with CAR structure (Besag et al. 1991), where the precision matrix was scaled such that the geometric mean of marginal variances was equal to one (Riebler et al. 2016). υ_i was added to the model to account for spatial structure in the model residuals (Dormann et al. 2007, Beale et al. 2010). β_0, β_1, β_2, and β_3 were given normal priors with mean = 0 and precision = 0.001. The prior for precision associated with the CAR term was a PC prior (Simpson et al. 2017) with parameter values $U_{pc} = 0.1$ and $a_{pc} = 0.01$.

Results

Analysis of the SVC model using R-INLA took approximately 10 minutes to complete. Inspection of the PIT histogram indicated satisfactory model fit. The median of posterior medians for α_i indicated that, on average, 4.28 robins were counted per party hour in 2017, but that number varied by several orders of magnitude across the species range, from 0.01 to 73.50.

A map of posterior median values illustrated that the species was most abundant in the central part of their range, and was least abundant along the northern and southern margins of their range (Fig. 1B).

Posterior median values for ϵ_i, the power law exponent for the relationship between effort and counts, varied from 0.28 to 1.44, with a median value of 0.81. The 95% credible intervals for ϵ_i values indicated that 80% of estimates were not significantly different from 1, while all were significantly greater than 0. Estimates not significantly different from 1 indicated a positive linear relationship between effort and counts. Values significantly greater than 0 and less than 1 also indicated a positive relationship between effort and counts, but one with diminishing returns for additional count effort. A map of posterior median ϵ_i values highlighted the spatial structure in the effort effect (Fig. 1C). Locations with posterior medians well below 1 were frequently locations with relatively low abundance indices (Fig. 1B), suggesting that the majority of robins in a count circle could be counted with relatively low effort. Locations with posterior medians closer to 1 were frequently locations with relatively high abundance indices (Fig. 1B), suggesting an endless supply of robins for CBC volunteers to count. The two parameters, α_i and ϵ_i, were significantly correlated across space, with a rank correlation coefficient of 0.26.

Posterior median values for τ_i, the temporal trend from 1966 through 2017, when transformed to annual percent change, varied from -11.80% to 13.63%, with a median value of 2.63% (Fig. 1D). The 95% credible intervals for τ_i values indicated that 8% of estimates were significantly lower than 0, while 44% were significantly greater than 0 (Fig. 1E). A map of posterior median τ_i values showed that relative abundance trends had strong spatial structure. Credible intervals for τ_i values (Fig. 1F) were used to illustrate where trends were significantly

negative or positive, showing that relative abundance during winter has generally decreased in the southern parts of their range and increased in the northern parts of their range. The parameters α_i and τ_i were significantly correlated across space, with a rank correlation coefficient of -0.16, indicating that the strongest trends were occurring at the margins of the geographic range where relative abundance was lowest.

The posterior median estimate for ϕ, the dispersion parameter, was $\exp[-\log(0.55)] = 1.83$, considerably larger than 1, highlighting overdispersion in robin counts relative to a Poisson distribution. Credible intervals for precision estimates for the random effects showed that all were important for explaining variation in the count data. When precision values were converted to a standard deviation scale, the random effects were ranked α_i (SD = 1.58), κ_k (1.05), ϵ_i (0.25), and τ_i (0.04), in terms of the amount of variation explained.

Figure 2 shows the median of posterior median SVC trends across cells per BCR (Fig. 2A), along with the posterior median trend for each BCR from the standard analysis (Fig. 2B). Side-by-side visual comparison of these maps showed that aggregate trends were similar, regardless of method. The SVC approach gave a median trend of 2.11 across all BCRs, while the posterior median trend for the standard approach was 1.95 across all BCRs. Within BCRs, the trend direction was consistent across the two methods in 28 of 32 BCRs. The rank correlation between BCR trends generated by the two methods was 0.88. Regarding differences, trends derived from the SVC approach changed more smoothly across the continent, as would be expected using a spatial statistical model. Also, the range of posterior median SVC trends (-4.58, 9.16) was slightly less than that for standard trends (-7.96, 14.26), especially near geographic range boundaries, as would be expected given the sharing of information across space.

Figure 3 compares the credible interval widths for SVC trends per grid cell (Fig. 3A) with those from the standard approach for aggregate BCR estimates (Fig. 3B). When compared to the standard approach, some SVC grid cells within a BCR, ones in information rich neighborhoods (Fig.1A), had SVC trend estimates with remarkably narrow confidence intervals (Fig. 3C, SVC minimum). Other grid cells, ones in information poor neighborhoods (Fig.1A), had trend estimates with relatively broad confidence intervals (Fig. 3C, SVC maximum). On average, however, precision of estimates per BCR were similar, regardless of method, if not slightly higher using the SVC approach (Fig. 3C, SVC median).

As predicted, SVC trends were positively related to degrees north latitude, with trends being negative at low latitudes and positive at high latitudes (Fig. 4A), suggesting a poleward shift in winter range for American Robins. After accounting for latitude, there was a clear negative relationship between mean minimum temperature and SVC trends (Fig. 4B), indicating that robins were becoming more abundant in historically colder areas at higher elevations and further from coasts. After accounting for latitude and minimum winter temperature, SVC trends were positively related to the number of people residing in a grid cell, which we use here as a proxy for resource availability for this anthropophilic species.

Discussion

This analysis demonstrated use of Bayesian SVC models to estimate long-term relative abundance trends in community science data collected at a continental scale. The inclusion of spatially structured random slope terms allowed for robust estimation of effort effects and relative abundance trends at spatial resolutions much finer than the standard analysis approach. The use of INLA for model analysis resulted in dramatically reduced computing time compared

to the standard analysis approach. Fine scaled trend estimates for the American Robin, when aggregated to the BCR level, were very similar to those produced by the standard analysis approach. When we explored correlates of American Robin SVC trends, we found that trends were related to latitude, winter temperature, and human population size as expected from the literature on factors governing the distribution and abundance of wintering birds.

To put resolution gains into context, consider that a CBC circle has a radius of approximately 12 km and an area of 452 km^2. A 100 km grid cell, covering 10,000 km^2, is approximate 22 times larger than a CBC circle. In comparison, the average analytical stratum has an area of 104,378 km^2, approximately 231 times the area of a CBC circle. Thus, the SVC approach brought an order of magnitude increase in spatial resolution when compared to the standard approach. This increased resolution is expected to facilitate finer scaled investigations into the drivers of winter bird trends (Thogmartin et al. 2004, Bled et al. 2013, Smith et al. 2015). Understanding the fine scale drivers of trends creates opportunities to tailor conservation plans to local conditions (Ethier and Nudds 2015, Ethier et al. 2017).

Estimating trends at relatively high resolution was made possible by adopting spatial statistical techniques designed to borrow information across neighboring regions (Thogmartin et al. 2004, Bled et al. 2013, Smith et al. 2015). Employing spatial techniques also had implications for uncertainty in trend estimates. In the standard analysis, the uncertainty in a trend estimate depended upon the variation in trends across the circles within a stratum and the number of circles in a stratum. In the SVC analysis, uncertainty depended upon those same two factors, but also depended upon those characteristics in the neighborhood of a grid cell. The consequences of this difference are demonstrated in Figure 3. In regions with many CBC circles (e.g., Piedmont BCR), SVC methods produced trend estimates with relatively low uncertainty

(minimum credible interval width of 1.48) compared to the standard method (3.40), due to the density of information. Similar to Bled et al. (2013), we found that precision of SVC estimates also tended to be relatively high in regions at the edge of a species range where there were few counts (e.g., Boreal Softwood Shield BCR, maximum interval width of 12.02) when compared to the standard approach (19.14), due to borrowing of information across neighboring cells that crossed regional boundaries. In other parts of the continent with fewer, more isolated CBC circles (e.g., Southern Rockies Colorado Plateau BCR), the SVC methods produced trend estimates with relatively high uncertainty (minimum interval width of 3.47) compared to the standard method (2.80). It is not entirely clear if the small intervals of the standard approach are justified in this context. If the relatively few and far-between circles that fall within those large BCRs can be considered representative samples of that larger area, then estimates with high precision are reasonable, and certainly preferred. If it cannot be assumed that those circles are representative of the larger area, then estimating trends for smaller areas, in neighborhoods with more information, and basing uncertainty estimates on the amount of local information, seems more appropriate. Critical evaluation of this representative-sample assumption is particularly important when analyzing data from the CBC, because count site selection is not based on sampling design principles, and count locations tend to be biased toward areas of high human population density and areas of high bird density and diversity (Drennan 1981, Dunn et al. 2005).

On a standard laptop computer, SVC model analysis using R-INLA took roughly 10 minutes for full Bayesian results. The standard approach, which employs MCMC, took approximately 10 hours for full Bayesian results on the same hardware. Had spatial statistical models been analyzed using MCMC, processing times would have been much longer. The difference in computing time was due to R-INLA producing highly accurate approximations of

Bayesian posteriors, orders of magnitude faster than MCMC (Rue et al. 2009, 2017). The obvious benefit of shorter processing times is that, for a given set of computing resources, more time periods, more distinct model forms (e.g., Link and Sauer 2016), or more species can be evaluated. Even small differences in computing time add up when analyzing counts from tens of years, for hundreds of species, across thousands of count sites.

There were, as there usually are, tradeoffs for rapid model analysis. Specifically, R-INLA is an analysis option whenever a statistical model can be expressed as a latent Gaussian model (Blangiardo et al. 2013, Rue et al. 2017). This was possible for the model used in this analysis. However, this would not have been possible had we chosen to use the effort-correction function developed by Link and Sauer (1999, 2006) and used in the standard analysis (Soykan et al. 2016). Here, we used a single-parameter, power-law function for effort correction because it could fit positive, negative, linear, increasing, and decreasing relationships (Butcher and McCulloch 1988) and was easily built into a latent Gaussian model. In contrast, the effort-correction function used for the standard approach is a two-parameter nonlinear function, which is more flexible and so will better-fit relationships that come to a rapid asymptote. Ideally, we would have tools for rapid analysis of spatial statistical models that incorporate the standard effort-correction function. In this choose-two situation, we erred towards rapid analysis of a spatial model with the simpler effort-correction function, because it allowed for more robust, if occasionally slightly biased (Link and Sauer 1999), estimates of the effort effect in regions where information was sparse. Robust estimates of effort effects are particularly critical when generating trends from CBC data, as count effort varies widely across time and space (Bock and Root 1981, Butcher et al. 1990, Dunn et al. 2005).

We note that the SVC approach described here differed from the standard approach in that it was optimized, specifically, for computing long-term, log-linear trends in relative abundance at fine spatial scales. The emphasis on long-term, log-linear trends was motivated by requests from resource managers, who desire simple summary statistics that reflect overall population status for many species (Rosenberg et al. 2016, 2017). The emphasis on fine spatial resolution was motivated by requests from, both, researchers wishing to conduct research at relatively fine spatial scales, and Audubon Christmas Bird Count volunteers, who wish to learn how bird numbers have changed over the years in their local area. Given these two emphases, we did not incorporate additional model terms necessary for creating annual abundance indices. These indices are critical for those who wish to look beyond single, long-term trends, at detailed time series that give more information about the nature of abundance changes (Sauer and Link 2002, 2011). Creating these annual indices is done by adding an additional random effect per cell and year, and combining these effects with α and τ. Adding this effect to the SVC model is easily done in R-INLA. This effect could be specified as exchangeable, or have spatial or temporal structure. For this dataset, preliminary trials showed that adding an exchangeable effect to the model increased computing time to approximately 1 hour. We did not explore this model variant in depth because producing annual abundance indices was not a primary goal of this effort.

When we applied the SVC approach to data from the American Robin, we learned that aggregate trends resulting from the SVC and standard approaches were similar in direction and magnitude. Precision at aggregate levels was generally similar, if not a bit lower with the SVC approach, due to different assumptions about how precision should, or should not, be related to the spatial distribution of counts. Spatial variation in SVC trends for the American Robin were

also consistent with expectations from the literature on factors governing winter bird distribution and abundance (Root 1988, Meehan et al. 2004, La Sorte and Thompson 2007, Zuckerberg et al. 2011). Specifically, trends were negative at low latitudes, positive at high latitudes and, for a given latitude, were more positive in historically cold regions and in areas with higher human population density. While it is likely that latitudinal effects would have been found using aggregate trends from the standard analysis (Fig. 2), it is less likely that residual winter temperature and human population density effects would have been detected. This is because winter temperatures and human population sizes both tend to vary at spatial scales considerably finer than an analytical strata, states, provinces or BCRs. Future studies could explore relationships between SVC trends and other potential variables that can be summarized at comparable spatial scales, such as forest management practices, agricultural intensification, and other factors related to land use and land cover.

Acknowledgements

We thank people. Good people.

Literature Cited

Banerjee, S., B. P. Carlin, and A. E. Gelfand (2014). Hierarchical Modeling and Analysis for Spatial Data. CRC Press, Boca Raton, Florida.

Beale, C. M., J. J. Lennon, J. M. Yearsley, M. J. Brewer, and D. A. Elston (2010). Regression analysis of spatial data. Ecology Letters 13:246–264.

Beissinger, S. R., and D. R. Osborne (1982). Effects of urbanization on avian community organization. Condor:75–83.

Besag, J., J. York, and A. Mollié (1991). Bayesian image restoration, with two applications in spatial statistics. Annals of the Institute of Statistical Mathematics 43:1–59.

Blangiardo, M., M. Cameletti, G. Baio, and H. Rue (2013). Spatial and spatio-temporal models with R-INLA. Spatial and Spatio-Temporal Epidemiology 7:39–55.

Bled, F., J. Sauer, K. Pardieck, P. Doherty, and J. A. Royle (2013). Modeling trends from North American Breeding Bird Survey data: a spatially explicit approach. PLoS ONE 8:e81867.

Bock, C. E., and T. L. Root (1981). The Christmas Bird Count and avian ecology. Studies in Avian Biology 6:17–23.

Butcher, G. S., M. R. Fuller, L. S. McAllister, and P. H. Geissler (1990). An evaluation of the Christmas Bird Count for monitoring population trends of selected species. Wildlife Society Bulletin 18:129–134.

Butcher, G. S., and C. E. McCulloch (1988). The influence of observer effort on the number of individual birds recorded on Christmas Bird Counts. In Survey Designs and Statistical Methods for the Estimation of Avian Population Trends (Sauer, J. R. and Droege, S., Editors). Biological Report 90:120–129.

CIESIN (2016). Gridded Population of the World, Version 4 (GPWv4): Population Count. Center for International Earth Science Information Network.

CIESIN (2017). Global Population Count Grid Time Series Estimates. Center for International Earth Science Information Network.

Congdon, P. (2014). Applied Bayesian Modelling. John Wiley & Sons.

Czado, C., T. Gneiting, and L. Held (2009). Predictive model assessment for count data. Biometrics 65:1254–1261.

Dawid, A. P. (1984). Statistical theory: the prequential approach. Journal of the Royal Statistical Society. Series A (General):278–292.

Dickinson, J. L., B. Zuckerberg, and D. N. Bonter (2010). Citizen science as an ecological research tool: challenges and benefits. Annual review of ecology, evolution, and systematics 41:149–172.

Dormann, C. F., J. M. McPherson, M. B. Araujo, R. Bivand, J. Bolliger, G. Carl, R. G. Davies, A. Hirzel, W. Jetz, W. D. Kissling, I. Kuhn, et al. (2007). Methods to account for spatial autocorrelation in the analysis of species distributional data: a review. Ecography 30:609–628.

Drennan, S. R. (1981). The Christmas Bird Count: an overlooked and underused sample. Studies in avian biology 6:24–29.

Dunn, E. H., C. M. Francis, P. J. Blancher, S. R. Drennan, M. A. Howe, D. Lepage, C. S. Robbins, K. V. Rosenberg, J. R. Sauer, and K. G. Smith (2005). Enhancing the scientific value of the Christmas Bird Count. The Auk 122:338–346.

Dunning, J. B., and J. H. Brown (1982). Summer rainfall and winter sparrow densities: a test of the food limitation hypothesis. Auk 99:123–129.

Ethier, D. M., N. Koper, and T. D. Nudds (2017). Spatiotemporal variation in mechanisms driving regional-scale population dynamics of a Threatened grassland bird. Ecology and Evolution 7:4152–4162.

Ethier, D. M., and T. D. Nudds (2015). Scalar considerations in population trend estimates: Implications for recovery strategy planning for species of conservation concern. The Condor 117:545–559.

Finley, A. O. (2011). Comparing spatially-varying coefficients models for analysis of ecological data with non-stationary and anisotropic residual dependence. Methods in Ecology and Evolution 2:143–154.

Gelfand, A. E., H.-J. Kim, C. F. Sirmans, and S. Banerjee (2003). Spatial modeling with spatially varying coefficient processes. Journal of the American Statistical Association 98:387–396.

Gneiting, T., and A. E. Raftery (2007). Strictly proper scoring rules, prediction, and estimation. Journal of the American Statistical Association 102:359–378.

Harris, I., P. D. Jones, T. J. Osborn, and D. H. Lister (2014). Updated high-resolution grids of monthly climatic observations–the CRU TS3. 10 Dataset. International journal of climatology 34:623–642.

Held, L., B. Schrödle, and H. avard Rue (2010). Posterior and cross-validatory predictive checks: a comparison of MCMC and INLA. In Statistical modelling and regression structures. Springer, pp. 91–110.

Hochachka, W. M., D. Fink, R. A. Hutchinson, D. Sheldon, Wong, Weng-Keen, and S. Kelling (2012). Data-intensive science applied to broad-scale citizen science. Trends in Ecology & Evolution 27:130–137.

Linden, A., and S. Mantyniemi (2011). Using the negative binomial distribution to model overdispersion in ecological count data. Ecology 92:1414–1421.

Lindgren, F., and H. Rue (2015). Bayesian spatial modelling with R-INLA. Journal of Statistical Software 63:19.

Link, W. A., and J. R. Sauer (1999). Controlling for varying effort in count surveys: an analysis of Christmas Bird Count data. Journal of Agricultural, Biological, and Environmental Statistics 4:116–125.

Link, W. A., and J. R. Sauer (2002). A hierarchical analysis of population change with application to Cerulean Warblers. Ecology 83:2832–2840.

Link, W. A., and J. R. Sauer (2016). Bayesian cross-validation for model evaluation and selection, with application to the North American Breeding Bird Survey. Ecology 97:1746–1758.

Link, W. A., J. R. Sauer, and D. K. Niven (2006). A hierarchical model for regional analysis of population change using Christmas Bird Count data, with application to the American Black Duck. The Condor 108:13–24.

Link, W. A., J. R. Sauer, and D. K. Niven (2017). Model selection for the North American Breeding Bird Survey: A comparison of methods. The Condor 119:546–556.

Marzluff, J. M. (1997). Effects of urbanization and recreation on songbirds. In: Block, William M.; Finch, Deborah M.(Tech. eds.). Songbird ecology in southwestern ponderosa pine forests: a literature review. Gen. Tech. Rep. RM-292. Fort Collins, CO: US Dept. of Agriculture, Forest Service, Rocky Mountain Forest and Range Experiment Station. p. 89-102. 292:89–102.

Meehan, T. D., W. Jetz, and J. H. Brown (2004). Energetic determinants of abundance in winter landbird communities. Ecol Lett Ecol Lett 7:532–537.

Niven, D. K., J. R. Sauer, G. S. Butcher, and W. A. Link (2004). Christmas Bird Count provides insights into population change in land birds that breed in the boreal forest. American Birds 58:10–20.

Pettit, L. I. (1990). The conditional predictive ordinate for the normal distribution. Journal of the Royal Statistical Society. Series B (Methodological):175–184.

Princé, K., and B. Zuckerberg (2015). Climate change in our backyards: the reshuffling of North America's winter bird communities. Global Change Biology 21:572–585.

Riebler, A., S. H. Sørbye, D. Simpson, and H. avard Rue (2016). An intuitive Bayesian spatial model for disease mapping that accounts for scaling. Statistical methods in medical research 25:1145–1165.

Robb, G. N., R. A. McDonald, D. E. Chamberlain, and S. Bearhop (2008). Food for thought: supplementary feeding as a driver of ecological change in avian populations. Frontiers in Ecology and the Environment 6:476–484.

Robbins, C. S., J. R. Sauer, R. S. Greenberg, and S. Droege (1989). Population declines in North American birds that migrate to the neotropics. Proceedings of the National Academy of Sciences 86:7658–7662.

Root, T. (1988). Energy constraints on avian distributions and abundances. Ecology 69:330–339.

Rosenberg, K. V., P. J. Blancher, J. C. Stanton, and A. O. Panjabi (2017). Use of North American Breeding Bird Survey data in avian conservation assessments. The Condor 119:594–606.

Rosenberg, K. V., J. A. Kennedy, R. Dettmers, R. P. Ford, D. Reynolds, J. D. Alexander, C. J. Beardmore, P. J. Blancher, R. E. Bogart, and G. S. Butcher (2016). Partners in flight landbird conservation plan: 2016 revision for Canada and continental United States. Partners in Flight Science Committee.

Rue, H., S. Martino, and N. Chopin (2009). Approximate Bayesian inference for latent Gaussian models by using integrated nested Laplace approximations. Journal of the Royal Statistical Society: Series B (Statistical Methodology) 71:319–392.

Rue, H., A. Riebler, S. H. Sørbye, J. B. Illian, D. P. Simpson, and F. K. Lindgren (2017). Bayesian computing with INLA: a review. Annual Review of Statistics and Its Application 4:395–421.

Sauer, J. R., J. E. Fallon, and R. Johnson (2003). Use of North American Breeding Bird Survey data to estimate population change for bird conservation regions. The Journal of Wildlife Management 67:372–389.

Sauer, J. R., and W. A. Link (2002). Using Christmas Bird Count data in analysis of population change. American Birds:10–14.

Sauer, J. R., and W. A. Link (2011). Analysis of the North American Breeding Bird Survey using hierarchical models. The Auk 128:87–98.

Sauer, J. R., K. L. Pardieck, D. J. Ziolkowski Jr, A. C. Smith, M.-A. R. Hudson, V. Rodriguez, H. Berlanga, D. K. Niven, and W. A. Link (2017). The first 50 years of the North American Breeding Bird Survey. The Condor 119:576–593.

Smith, A. C., M.-A. R. Hudson, C. M. Downes, and C. M. Francis (2015). Change points in the population trends of aerial-insectivorous birds in North America: synchronized in time across species and regions. PLOS ONE 10:e0130768.

La Sorte, F. A., and F. R. Thompson (2007). Poleward Shifts in Winter Ranges of North American Birds. Ecology 88:1803–1812.

Soykan, C. U., J. Sauer, J. G. Schuetz, G. S. LeBaron, K. Dale, and G. M. Langham (2016). Population trends for North American winter birds based on hierarchical models. Ecosphere 7:e01351.

Thogmartin, W. E., J. R. Sauer, and M. G. Knutson (2004). A hierarchical spatial model of avian abundance with application to Cerulean Warblers. Ecological Applications 14:1766–1779.

Thomas, C. D., and J. J. Lennon (1999). Birds extend their ranges northwards. Nature 399:213.

Waller, L. A., and C. A. Gotway (2004). Applied Spatial Statistics for Public Health Data. John Wiley & Sons, New York, NY.

Zuckerberg, B., D. N. Bonter, W. M. Hochachka, W. D. Koenig, A. T. DeGaetano, and J. L. Dickinson (2011). Climatic constraints on wintering bird distributions are modified by urbanization and weather: Wintering birds, weather, food, and climate. Journal of Animal Ecology 80:403–413.

Supplemental Information

All code and data needed to reproduce the SVC analysis is available at

https://github.com/tmeeha/inlaSVCBC.

Figure Captions

Figure 1. Select inputs and outputs to the SVC model, including: (A) a map of the grid cell structure used in the American Robin analysis, along with the number of CBC circles included in each cell; (B) α_i, representing the relative abundance index for 2017; (C) ϵ_i, representing the effort-effect exponent; (D, E) τ_i, representing the long-term log-linear trend as percent change per year per grid cell. Note that values shown in E are significantly different from 0, based on (E) 95% credible intervals for τ_i.

Figure 2. Comparison of posterior median trends for American Robin, aggregated to Bird Conservation Regions, produced by (A) SVC and (B) standard methods, showing spatial variation in their relationships and their pairwise correlation (C). The dark grey diagonal line in C represents equality.

Figure 3. Comparison of 95% credible interval widths for (A) estimates of τ_i (Tau, long-term log-linear trend, percent change per year per grid cell) from the American Robin SVC model and (B) analogous trends produced using the standard analysis and aggregated to Bird Conservation Regions, shown as maps and (C) summarized with box plots.

Figure 4. Model predictions and 95% credible intervals illustrating associations between American Robin SVC trends and (A) degrees north Latitude, (B) mean minimum winter temperature between 1965 and 2017, and (C) mean human population size between 1971 and 2015.

Figure 1

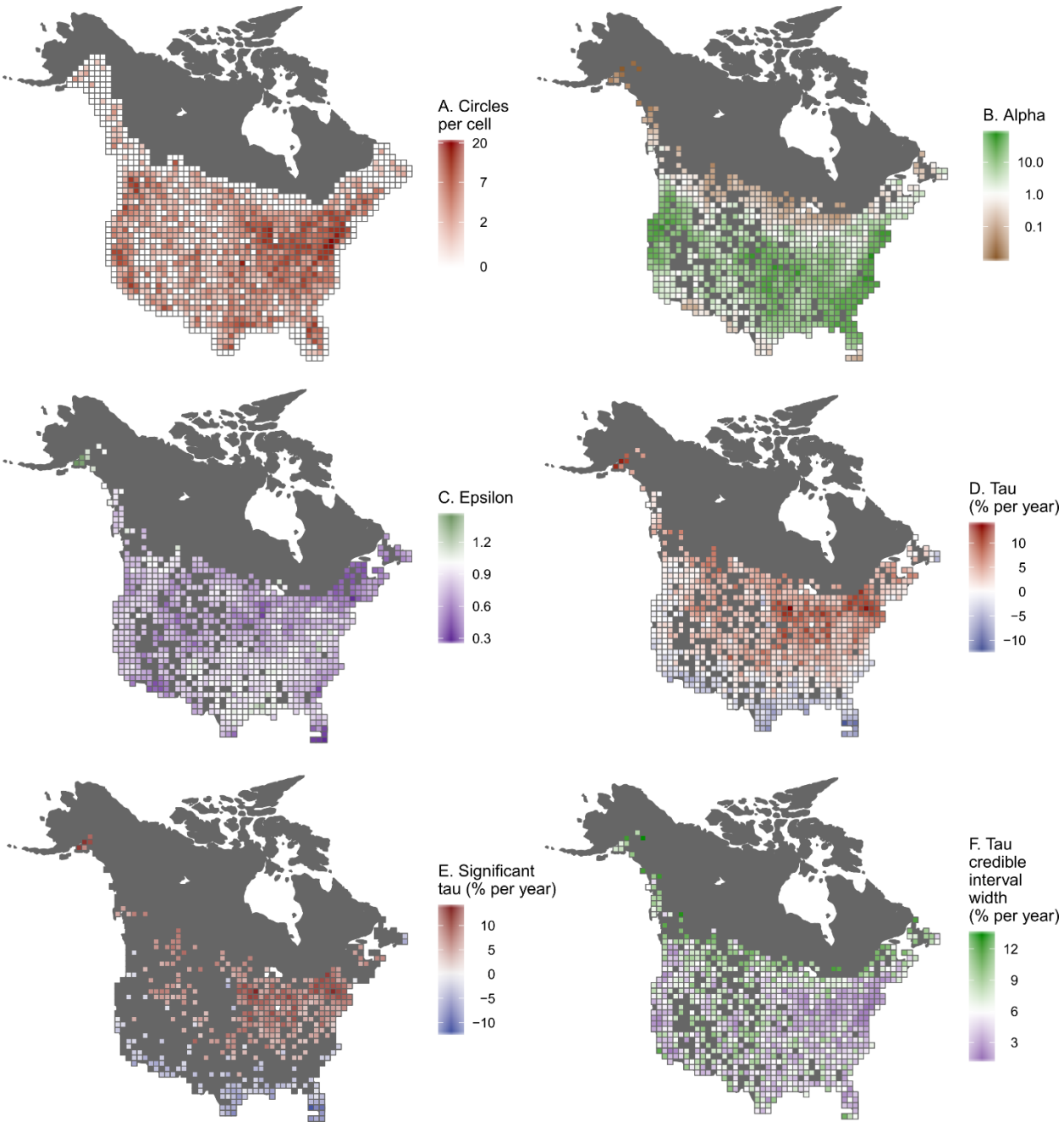
A. Circles per cell
20
7
2
0
B. Alpha
10.0
1.0
0.1
C. Epsilon
1.2
0.9
0.6
0.3
D. Tau (% per year)
10
5
0
−5
−10
E. Significant tau (% per year)
10
5
0
−5
−10
F. Tau credible interval width (% per year)
12
9
6
3

Figure 2

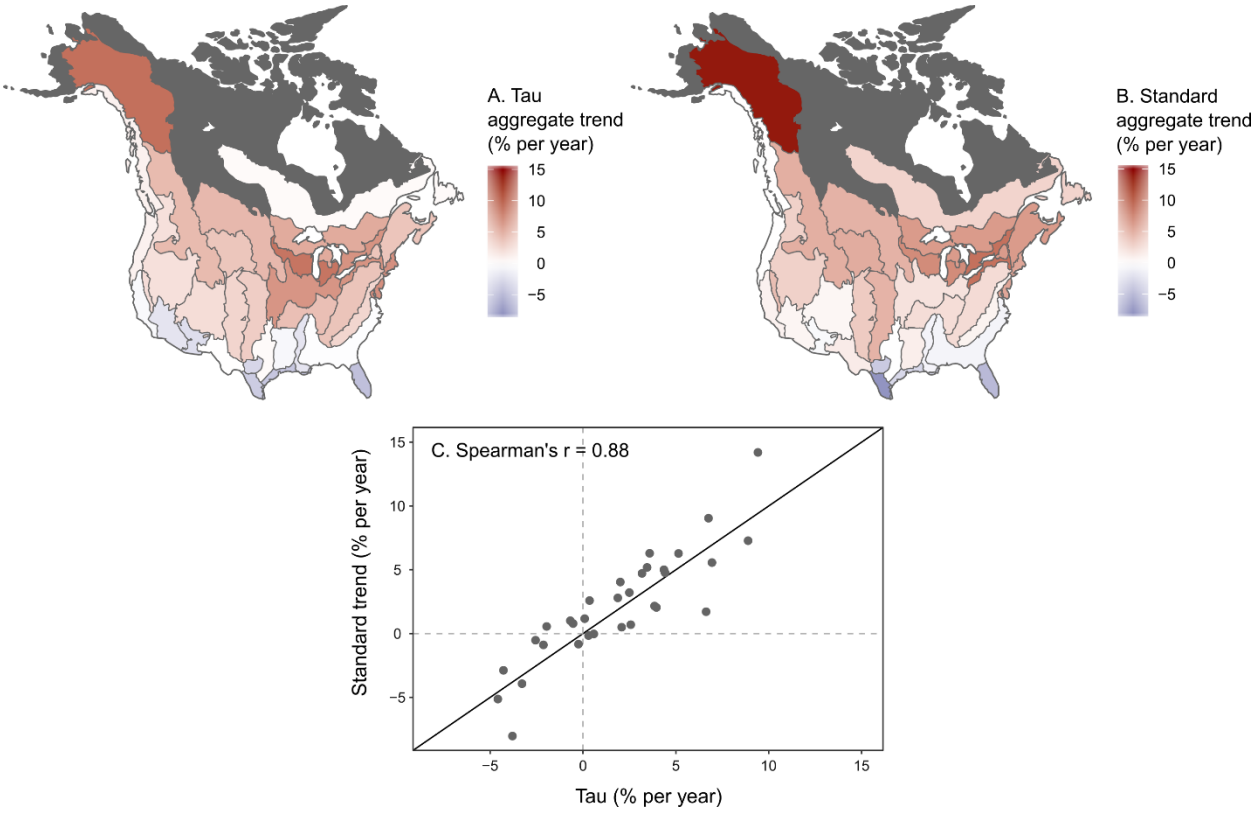
A. Tau
aggregate trend
(% per year)
15
10
5
0
−5
B. Standard
aggregate trend
(% per year)
15
10
5
0
−5
C. Spearman's r = 0.88
Standard trend (% per year)
Tau (% per year)
15
10
5
0
−5
−5
0
5
10
15

Figure 3.

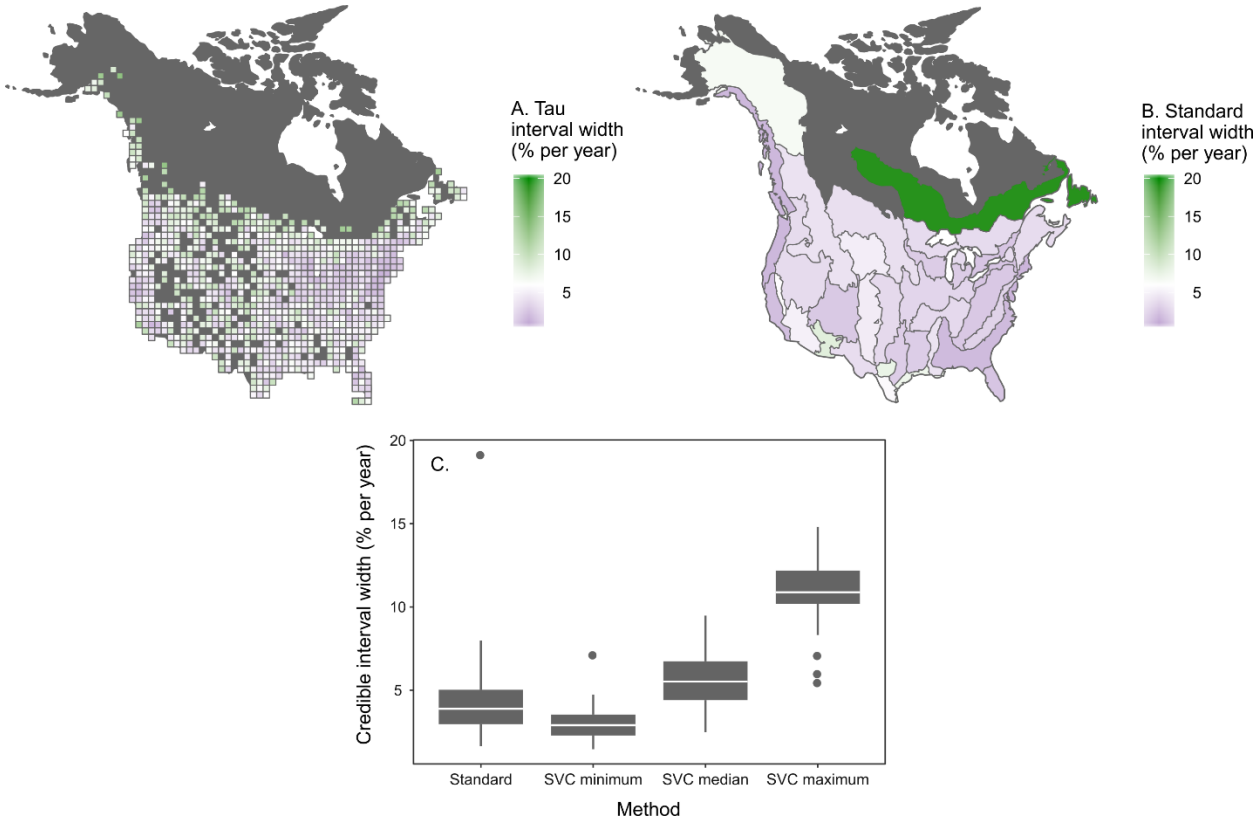
A. Tau
interval width
(% per year)
20
15
10
5
B. Standard
interval width
(% per year)
20
15
10
5
C.
Credible interval width (% per year)
20
15
10
5
Standard
SVC minimum
SVC median
SVC maximum
Method

Figure 4.

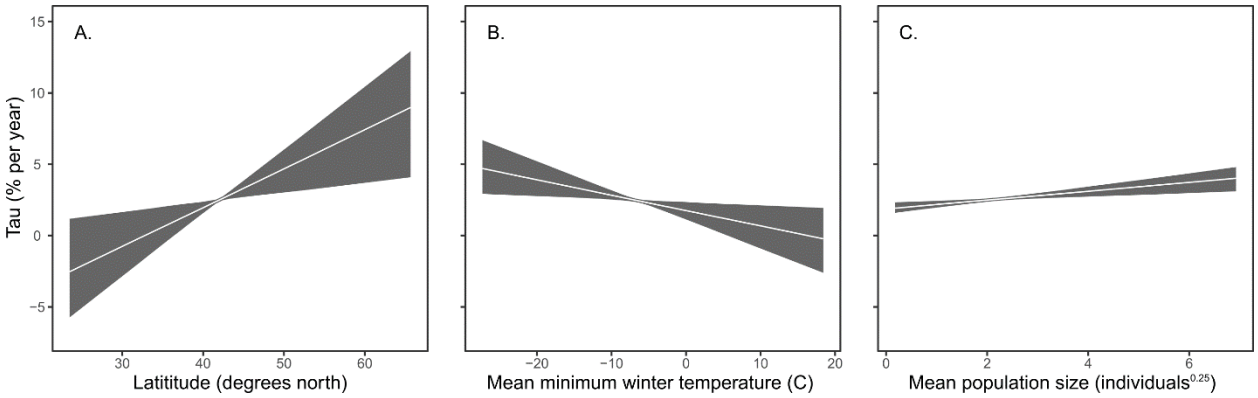
A.
B.
C.
Tau (% per year)
15
10
5
0
−5
30
40
50
60
Latititude (degrees north)
−20
−10
0
10
20
Mean minimum winter temperature (C)
0
2
4
6
Mean population size (individuals$^{0.25}$)